Adaptive Control for the Conventional Mode of Operation of MEMS Gyroscopes

Sungsu Park, *Member, IEEE,* and Roberto Horowitz, *Member, IEEE, Member, ASME*

***Abstract*—This paper presents adaptive add-on control algorithms for the conventional mode of operation of MEMS z-axis gyroscopes. This scheme is realized by adding an outer loop to a conventional force-balancing scheme that includes a parameter estimation algorithm. The parameter adaptation algorithm estimates the angular rate, identifies and compensates the quadrature error, and may permit on-line automatic mode tuning. The convergence and resolution analysis show that the proposed adaptive add-on control scheme prevents the angular rate estimate from being contaminated by the quadrature error, while keeping ideal resolution performance of a conventional force-balancing scheme. [838]**

***Index Terms*—Adaptive control, averaging analysis, force-balancing control, gyroscope, MEMS.**

I. Introduction

MOST MEMS gyroscopes are vibratory rate gyroscopes that have structures fabricated on polysilicon or crystal silicon, and mechanical main component is a two degree-of-freedom vibrating structure, which is capable of oscillating on two directions in a plane. Their operating physics is based on the Coriolis effect. When the gyroscope is subjected to an angular velocity, the Coriolis effect transfers energy from one vibrating mode to another. The response of the second vibrating mode provides information about the applied angular velocity. Ideally in the conventional mode of operation, the vibrating modes of a MEMS gyroscope are supposed to remain mechanically uncoupled, their natural frequencies should be matched, and the gyroscope's output should only be sensitive to angular velocity. In practice however, fabrication imperfections and environment variations are always present, resulting in a frequency of oscillation mismatch between the two vibrating modes and a coupling between the two mechanical vibration modes through off-diagonal terms in the stiffness and damping matrices. These imperfections degrade the gyroscope's performance and cause a false output [1], [2]. As a consequence, some kind of control is essential for improving the performance and stability of MEMS gyroscopes, by effectively cancelling "parasitic" effects.

Manuscript received march 28, 2002; revised September 5, 2002. This work was supported by DARPA under Contract N66001-97-C-8643. Subject Editor G. B. Hocker.

S. Park is with the PATH, University of California at Berkeley, Berkeley, CA 94720 USA and also with the Berkeley Sensor and Actuator Center, Department of Mechanical Engineering, University of California at Berkeley, and 1357 South 46th Street, Bldg. 452, Richmond, CA 94804 USA (email: sungsu@path.berkeley.edu).

R. Horowitz is with the Department of Mechanical Engineering, University of California at Berkeley, Berkeley, CA 94720 USA (email: horowitz@me.berkeley.edu).

Digital Object Identifier 10.1109/JMEMS.2002.807468

Traditionally, mechanical or electrical balancing has been used to cancel parasitic effects [3]–[5]. Although this procedure reduces the effect of a certain amount of imperfections, it is time consuming, expensive and difficult to perform on small, nail-size (mm level) gyroscopes. An open-loop scheme [3] and a feedback controller [6] for the quadrature error compensation were proposed for an open-loop mode of operation. Both of these methods utilize the fact that the responses of the Coriolis acceleration and the quadrature error are 90 degree out-of-phase with respect to each other. For a closed-loop mode of operation, two feedback control methods have been presented in the literature that compensate fabrication imperfections and measure angular velocity. One is a Kalman filter based preview control [7] and the others are force-balancing feedback control schemes [8], [9]. Although these feedback control techniques increase the bandwidth and dynamic range of the gyroscope beyond the open-loop mode of operation, they still are sensitive to parameter variations, and angular rate estimate may be contaminated by the quadrature error.

In this paper, we develop an adaptive add-on control scheme for operating a MEMS z-axis gyroscope in conventional force-balancing mode. This adaptive algorithm estimates the angular rate and, at the same time, identifies and compensates quadrature error, and may permit on-line automatic mode tuning. In the next sections, the dynamics of MEMS gyroscopes is developed and analyzed, by accounting for the effect of fabrication imperfections. The closed-loop mode of operation is reviewed in Section III. In Section IV, an adaptive add-on control approach is developed as an extension of conventional force-balancing control scheme, and the convergence and resolution analysis of the proposed adaptive add-on controlled gyroscope is presented. Finally, computer simulations are performed in Section V.

II. Dynamics of MEMS Gyroscopes

Common MEMS vibratory gyroscope configurations include a proof mass suspended by spring suspensions, and electrostatic actuations and sensing mechanisms for forcing an oscillatory motion and sensing the position and velocity of the proof mass. These mechanical components can be modeled as a mass, spring and damper system. Fig. 1 shows a simplified model of a MEMS gyroscope having two degrees of freedom in the associated Cartesian reference frames. Assuming that the motion of the proof mass is constrained to be only along the $x-y$ plane by making the spring stiffness in the z direction much larger than in the x and y directions, the measured angular rate is almost constant over a long enough time interval, and linear accelerations are cancelled out, either as an offset from the output response or

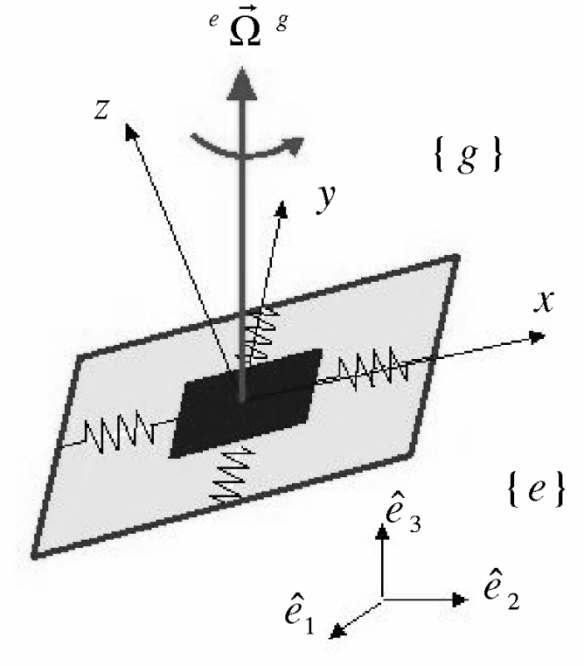

Fig. 1. Model of a MEMS z-axis gyroscope.

by applying counter-control forces, then the equation of motion of a gyroscope is simplified as follows.

$$m\ddot{x}+d_1\dot{x}+(k_1-m(\Omega_y^2+\Omega_z^2))x+m\Omega_x\Omega_y y=\tau_x+2m\Omega_z\dot{y}$$
$$m\ddot{y}+d_2\dot{y}+(k_2-m(\Omega_x^2+\Omega_z^2))y+m\Omega_x\Omega_y x=\tau_y-2m\Omega_z\dot{x} \quad (1)$$

where x and y are the coordinates of the proof mass relative to the gyro frame, $d_{1,2}$, $k_{1,2}$ are damping and spring coefficients, $\Omega_{x,y,z}$ are the angular velocity components along each axis of the gyro frame, and $\tau_{x,y}$ are control forces. The two last terms in (1), $2m\Omega_z\dot{x}$ and $2m\Omega_z\dot{y}$, are due to the Coriolis forces and are the terms which are used to measure the angular rate Ω_z.

As seen in (1), in an ideal gyroscope, only the component of the angular rate along the z-axis, Ω_z, causes a dynamic coupling between the x and y axes, under the assumption that $\Omega_{x,y}^2 \approx \Omega_x\Omega_y \approx 0$. In practice, however, small fabrication imperfections always occur, and also cause dynamic coupling between the x and y axes through the asymmetric spring and damping terms. Taking into account fabrication imperfections, the dynamic (1) are modified as follows [10].

$$m\ddot{x}+d_{xx}\dot{x}+d_{xy}\dot{y}+k_{xx}x+k_{xy}y=\tau_x+2m\Omega_z\dot{y}$$
$$m\ddot{y}+d_{xy}\dot{x}+d_{yy}\dot{y}+k_{xy}x+k_{yy}y=\tau_y-2m\Omega_z\dot{x}. \quad (2)$$

Equation (2) is the governing equation for a MEMS z-axis gyroscope. Fabrication imperfections contribute mainly to the asymmetric spring and damping terms, k_{xy} and d_{xy}. Therefore these terms are unknown, but can be assumed to be small. The x and y axes spring and damping terms are mostly known, but have small unknown variations from their nominal values. The proof mass can be determined very accurately. The components of angular rate along x and y axes are absorbed as part of the spring terms as unknown variations. Note that the spring coefficients k_{xx} and k_{yy} also include the electrostatic spring softness.

Based on m, q_0 and ω_0, which are a reference mass, length and natural resonance frequency respectively, where m is a proof mass of the gyroscope, the nondimensionalization of (2) can be done as follows [11]:

$$\ddot{x}+\frac{\omega_x}{Q_x}\dot{x}+d_{xy}\dot{y}+\omega_x^2 x+\omega_{xy}y=\tau_x+2\Omega_z\dot{y}$$
$$\ddot{y}+d_{xy}\dot{x}+\frac{\omega_y}{Q_y}\dot{y}+\omega_{xy}x+\omega_y^2 y=\tau_y-2\Omega_z\dot{x} \quad (3)$$

where Q_x and Q_y are respectively the x and y axis quality factor, $\omega_x=\sqrt{k_{xx}/(m\omega_0^2)}$, $\omega_y=\sqrt{k_{yy}/(m\omega_0^2)}$, $\omega_{xy}=k_{xy}/(m\omega_0^2)$, $d_{xy} \leftarrow d_{xy}/(m\omega_0)$, $\Omega_z \leftarrow \Omega_z/\omega_0$, $\tau_x \leftarrow \tau_x/(m\omega_0^2 q_0)$, and $\tau_y \leftarrow \tau_y/(m\omega_0^2 q_0)$.

III. Closed-Loop Mode of Operation

A. Strategy and Previous Work

Conventional mode of operation is classified by an open-loop mode and a closed-loop mode. The measurement strategy of both the open-loop and closed-loop modes is based on the same physics, i.e. generating a Coriolis acceleration by driving a proof mass in a constant amplitude oscillation along the drive axis and inducing an oscillation along the sense axis, which is proportional to the applied angular rate. The major difference between the closed-loop and open-loop mode of operation lies in that in the former the displacement of the sense axis is controlled to zero, while in the latter it is measured. The benefits of a closed-loop operation are more scale factor stability, higher linearity and higher bandwidth, thus achieving better performance than that in the open-loop mode of operation. However, the effect of the asymmetric damping term is not distinguishable from the Coriolis acceleration term. Thus, this term still creates an inherent zero-rate output as in the case of the open-loop mode of operation. The process of conventional mode of operation is based on the following equation:

$$x=X_0\sin(\omega_x t)$$
$$\ddot{y}+\frac{\omega_y}{Q_y}\dot{y}+\omega_y^2 y=\tau_y-\omega_{xy}x-(d_{xy}+2\Omega_z)\dot{x} \quad (4)$$

where X_0 is the amplitude of x-axis oscillation.

B. Force-Balancing Control

The force-balancing control strategy was originally developed for MEMS accelerometer control [12], where it has been successfully applied, and it has been extended to MEMS gyroscopes [8], [9]. The basic idea behind the force-balancing control strategy is that, if the sense mode amplitude is regulated to zero by feedback control action, then, since $\ddot{y} \approx \dot{y} \approx y \approx 0$, (4) yields in steady-state response,

$$\tau_y=\omega_{xy}x+(d_{xy}+2\Omega_z)\dot{x}. \quad (5)$$

This implies that applied angular rate Ω_z can in principle be inferred from the sense axis control output τ_y, under the assumption that $d_{xy}=0$. The force-balancing control strategy requires that the sense axis closed loop system be robust to parameter uncertainties and variations, and have minimal phase shift so that the response of the system to the Coriolis acceleration and quadrature error can be distinguishable. A block diagram of a sense axis force-balancing control is shown in Fig. 2. $G(s)$ is the sense axis gyroscope dynamics, $K(s)$ is

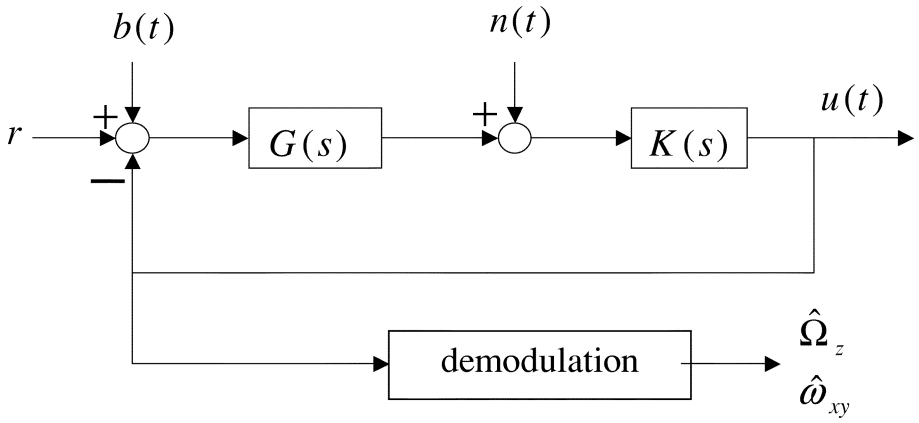

Fig. 2. Block diagram of the force-balancing control.

the compensator which will be subsequently designed, $r = -2\Omega_z\omega_x X_0\cos(\omega_x t) - \omega_{xy}X_0\sin(\omega_x t)$is the modulated input signal resulting from the Coriolis acceleration and quadrature error, $u = \tau_y$ is the control output, n is the measurement noise, and b is the Brownian input noise. Fig. 2 also includes a demodulation block, which will be defined subsequently. The closed loop sensitivity transfer functions for u and y are given by

$$\begin{aligned} u(s) &= T(s)(r+b) + S(s)n \\ y(s) &= V(s)(r+b) - T(s)n \end{aligned} \tag{6}$$

where

$$T(s) = \frac{K(s)G(s)}{1+K(s)G(s)},\ S(s) = \frac{K(s)}{1+K(s)G(s)}$$
$$V(s) = \frac{G(s)}{1+K(s)G(s)}.$$

The control design goal is to flatten the gain of the complementary sensitivity function $T(s)$ for u around the drive axis frequency ω_x, i.e.

$$|T(j\omega)| \approx const, \quad for\ \omega \in [\omega_x - \Delta\omega, \omega_x + \Delta\omega].$$

The compensator $K(s)$ may be designed by various methods such as μ-synthesis and H^∞ for stability robustness, or using classical control synthesis techniques. If the magnitude of the closed-loop complementary transfer function $T(s)$ from the angular rate to the control output is flat around the drive axis frequency, the gyroscope's scale factor will remain constant in the presence of drive or sense axis frequency variations. Moreover, the gyroscope's bandwidth can be increased up to the drive axis frequency. The dynamic range and linearity are also improved to the extent of the control authority, since the magnitude of the sensitivity transfer function $V(s)$ from the angular rate to the sense axis displacement is almost zero. Since, by (6), the steady-state control signal u contains both the Coriolis and quadrature error signals, a demodulation is needed for extracting angular velocity information from the control signal. Eventually, the overall gyroscope performance will depend on the demodulation method used.

The steady state response of the control output of (6) is given by

$$u(t) = u_{\mathrm{Cori}}(t) + u_{\mathrm{quad}}(t) + u_b(t) + u_n(t) \tag{7}$$

where

$$\begin{aligned} u_{Cori}(t) &= -X_0\omega_x\Omega_{z0}T_{\mathrm{Cori}\pm}\cos((\omega_x \pm \delta)t + \phi_{\mathrm{Cori}\pm}) \\ u_{\mathrm{quad}}(t) &= -X_0\omega_{xy}T_{\mathrm{quad}}\sin(\omega_x t + \phi_{quad}) \\ u_b &\sim \left(0, \sigma_b^2\right), u_n \sim \left(0, \sigma_n^2\right) \end{aligned}$$

and

$$\begin{aligned} T_{\mathrm{Cori}\pm} &= |T(s)|_{s=j(\omega_x\pm\delta)}, \quad T_{\mathrm{quad}} = |T(s)|_{s=j\omega_x} \\ \phi_{\mathrm{Cori}\pm} &= \angle(T(s))_{s=j(\omega_x\pm\delta)}, \quad \phi_{\mathrm{quad}} = \angle(T(s))_{s=j\omega_x} \end{aligned}$$

where it is assumed that $\Omega_z = \Omega_{z0}\cos(\delta t)$. Suppose that the phase delay is small, i.e. $\phi_{\mathrm{Cori,quad}} \approx 0$ around the anticipated drive frequency region. Then, the angular rate and quadrature error may be demodulated from the control output by multiplying this signal by $\cos(\omega_x t)$ and $\sin(\omega_x t)$, and filtering the resulting signals with a low-pass filter. The demodulated signals become

$$\begin{aligned} \hat{\Omega}_z &= F_{\mathrm{LPF}}(u(t)\cdot\cos(\omega_x t) \\ &= -\frac{1}{2}X_0\omega_x T_{\mathrm{Cori}\pm}\Omega_{z0}\cos(\pm\delta t + \phi_{\mathrm{Cori}\pm} + \phi_{\mathrm{LPF}}) \\ &\quad -\frac{1}{2}X_0\omega_{xy}T_{\mathrm{quad}}\sin(\phi_{\mathrm{quad}} + \phi_{\mathrm{LPF}}) + u_{bf} + u_{nf} \\ \hat{\omega}_{xy} &= F_{\mathrm{LPF}}(u(t)\cdot\sin(\omega_x t) \\ &= \frac{1}{2}X_0\omega_x T_{\mathrm{Cori}\pm}\Omega_{z0}\sin(\pm\delta t + \phi_{\mathrm{Cori}\pm} + \phi_{\mathrm{LPF}}) \\ &\quad -\frac{1}{2}X_0\omega_{xy}T_{\mathrm{quad}}\cos(\phi_{\mathrm{quad}} + \phi_{\mathrm{LPF}}) + u_{bf} + u_{nf} \end{aligned}$$

where ϕ_{LPF} is the phase delay due to the low-pass filter, $u_{bf} = F_{\mathrm{LPF}}(\cos(\omega_x t)\cdot u_b)$ and $u_{nf} = F_{\mathrm{LPF}}(\cos(\omega_x t)\cdot u_n)$. Notice however that, unless the ϕ_{quad} is exactly zero, the estimation of angular rate is contaminated by the unknown quadrature error coupling term ω_{xy}. Unfortunately, usually the quadrature error is three or four orders of magnitude larger than the angular rate. Although the quadrature error term can potentially be cancelled out by initial calibration, it may vary during the operation of the gyroscope. In the force-balancing approach, sense and drive resonance frequency mismatch is not as critical a problem as is in the open-loop operation, unless the gyroscope closed-loop bandwidth is much larger than in the open-loop mode. Fig. 3 explains this fact graphically. When high resolution is required, resonant mode matching is important to attain a consistent resolution performance. However, in this case the bandwidth of the gyroscope will be small. This is also the case in the open-loop

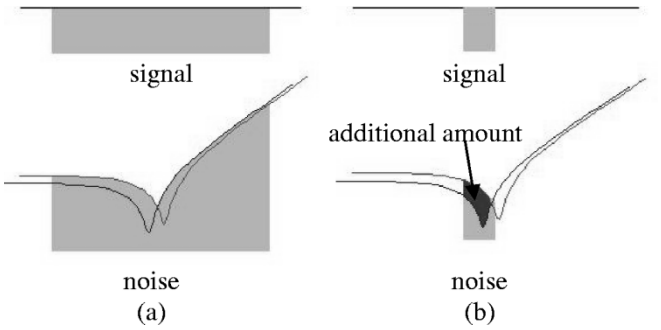

Fig. 3. Mode mismatch does not have large effect on the resolution of a large bandwidth system [see case (a)], but has a large effect on a small bandwidth system [see case (b)].

mode, where mode matching is important in order to attain a consistent scale factor. However, as opposed to the open-loop operation mode, it is very difficult to tune the sense axis resonant frequency, since phase information for mode matching is lost in closed-loop operation mode.

IV. Adaptive Add-on Control

We investigate the use of an adaptive algorithm for estimating angular rate and at the same time, identifying and compensating quadrature error, and possibly attaining mode match in an on-line fashion. Note that the effect of variations in drive or sense axis frequencies is not observed explicitly in the control output of a conventional force-balancing system. The idea behind the use of adaptive add-on control is to make the nominal control output of the conventional force-balancing system equal to zero by adding an additional outer loop. The add-on control outer loop is composed of a band-pass filter, a parameter adaptation law and a modulation part. Fig. 4 shows a block diagram of force-balancing system with the adaptive add-on control.

The modulated input signal r in the (6) is rewritten in regressor form as

$$r = -2\Omega_z\dot{x} - \omega_{xy}x = -\theta^T v \tag{8}$$

where $\theta = [2\Omega_z\ \omega_{xy}]^T$ is assumed to be an unknown parameter and $v = [\dot{x}\ x]^T$ is the measurable regressor. Suppose that the input signal r is estimated by a parameter adaptation algorithm, then its estimate signal and errors are

$$\begin{aligned}\hat{r} &= -2\hat{\Omega}_z(t)\dot{x} - \hat{\omega}_{xy}(t)x = -\hat{\theta}^T v\\ \tilde{r} &= r - \hat{r} = 2\tilde{\Omega}_z(t)\dot{x} + \tilde{\omega}_{xy}x = \tilde{\theta}^T v\end{aligned} \tag{9}$$

where the parameter estimate errors are $\tilde{\Omega}_z = \hat{\Omega}_z - \Omega_z$, $\tilde{\omega}_{xy} = \hat{\omega}_{xy} - \omega_{xy}$ and $\tilde{\theta} = \hat{\theta} - \theta$. The control error dynamics $\tilde{u}$ is

$$\begin{aligned}\tilde{u} &= T(r + b - \hat{r}) + S(n)\\ &= T(\tilde{\theta}^T v) + T(b) + S(n).\end{aligned} \tag{10}$$

If the error signal $\tilde{u}$ passes through a band-pass filter $F_{\mathrm{BPF}}(s)$, then

$$\begin{aligned}\tilde{u}_f &= F_{\mathrm{BPF}}(\tilde{u})\\ &= T_{\mathrm{BPF}}(\tilde{\theta}^T v) + T_{\mathrm{BPF}}(b) + S_{\mathrm{BPF}}(n)\end{aligned} \tag{11}$$

where $T_{\mathrm{BPF}}(s) = F_{\mathrm{BPF}}(s)T(s)$ and $S_{\mathrm{BPF}}(s) = F_{\mathrm{BPF}}(s)S(s)$. The following theorem holds.

Theorem 1: Assume that Ω_z and ω_{xy} are constant. Suppose that a conventional force-balancing closed loop system is stable with a controller $K(s)$. If a band-pass filter is designed such that the phase delay from the modulated input signal r to the output of a band-pass filter is less than 90° for a drive axis frequency ω_x, and the parameter estimates $\hat{\Omega}_z$ and $\hat{\omega}_{xy}$ are updated by the following adaptation laws:

$$\begin{aligned}\dot{\hat{\Omega}}_z &= -\gamma_\Omega \tilde{u}_f \dot{x}\\ \dot{\hat{\omega}}_{xy} &= -\gamma_\omega \tilde{u}_f x\end{aligned} \tag{12}$$

then the angular rate Ω_z and quadrature error ω_{xy} can be estimated correctly, i.e., $\tilde{\Omega}_z \to 0$, $\tilde{\omega}_{xy} \to 0$, where γ_Ω and γ_ω are positive adaptation gains.

Proof: Since the propagation equation of the stochastic expectation has the same form as the deterministic counterpart, we can consider the deterministic case, i.e. $b = 0$ and $n = 0$. Usually, $T(s)$ and $T_{\mathrm{BPF}}(s)$ are not SPR (strictly positive real), so it is difficult to prove the stability of the closed-loop system with an adaptation loop. Here, we make use of the fact that the driving signal is a single frequency sinusoid, and take an averaging approach [13]. Assuming that the applied angular rate and quadrature error are constant, then (12) is equal to

$$\dot{\tilde{\theta}} = -\begin{bmatrix} 2\gamma_\Omega & 0 \\ 0 & \gamma_\omega \end{bmatrix} \begin{bmatrix} X_0\omega_x\cos(\omega_x t) \\ X_0\sin(\omega_x t) \end{bmatrix} \tilde{u}_f. \tag{13}$$

Assuming that estimate error dynamics $\tilde{\theta}$ is slow, from (11), the steady-state dynamics of $\tilde{u}_f$ is approximately given by

$$\begin{aligned}\tilde{u}_f \approx\ & T_{\mathrm{BPF}}(v^T)\tilde{\theta} = |T_{\mathrm{BPF}}(\omega_x)|\\ &\times[X_0\omega_x\cos(\omega_x t + \phi)\ X_0\sin(\omega_x t + \phi)]\tilde{\theta}\end{aligned} \tag{14}$$

where ϕ is a phase delay from the modulated input signal r to the output of the band-pass filter. Substituting (14) into (13) and taking averages result in

$$\begin{bmatrix} \dot{\tilde{\Omega}}_z \\ \dot{\tilde{\omega}}_{xy} \end{bmatrix}_{AVG} = -|T_{BPF}(\omega_x)|X_0^2 R_{\Omega\omega} \begin{bmatrix} \tilde{\Omega}_z \\ \tilde{\omega}_{xy} \end{bmatrix}_{AVG} \tag{15}$$

where

$$R_{\Omega\omega} = \begin{bmatrix} \gamma_\Omega\omega_x^2\cos\phi & -\gamma_\Omega\omega_x\sin\phi \\ \frac{1}{2}\gamma_\omega\omega_x\sin\phi & \frac{1}{2}\gamma_\omega\cos\phi \end{bmatrix}.$$

We have used the fact that the products of sinusoids at different frequencies have zero average. A sufficient condition for the system in (15) to be asymptotically stable is that the cross-correlation matrix $R_{\Omega\omega}$ be positive-definite. This is achieved if $\cos\phi > 0$. Therefore, if $-90^\circ < \phi < 90^\circ$, the convergence of parameter errors to zero is guaranteed, and the stability of the system is proven. ■

If we carefully design a compensator $K(s)$ and a band-pass filter $F_{\mathrm{BPF}}(s)$ so that phase delay is as small as possible, the angular rate estimate dynamics will be almost decoupled from that of the quadrature error estimate. In this case, the quadrature error estimation transient response will not significantly affect the transient response of the angular rate estimate and vice versa. Although the quadrature error estimate dynamics affects that of the angular rate estimate, this only happens during the transient period. This is the main advantage of this scheme over the conventional force-balancing control, where the angular rate estimate is contaminated by the quadrature error term, unless it is perfectly compensated.

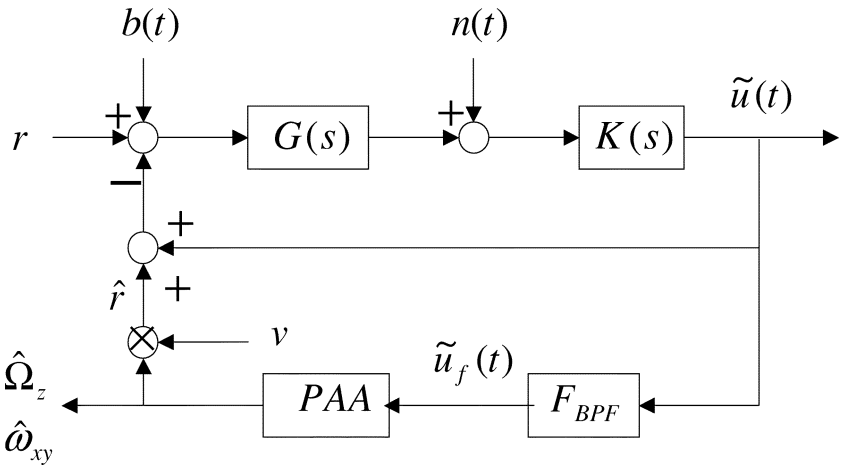

Fig. 4. Block diagram of the adaptive add-on control Parameter Adaptation Algorithm (PAA).

A. Performance Expectation

The bandwidth of a conventional force-balancing controlled gyroscope is defined by the cutoff frequency of the low-pass filter used in the demodulation process. On the other hand, the bandwidth of the proposed force-balancing controlled gyroscope with adaptive add-on control is defined by the adaptation gain γ_Ω. From (15), assuming that $\phi \approx 0$, its bandwidth can be estimated by

$$BW \approx \gamma_\Omega |T_{BPF}(\omega_x)| X_0^2 \omega_x^2. \tag{16}$$

Of course, the actual maximum bandwidth is also limited by the band-pass filter. Therefore, the adaptation gain γ_Ω should be selected so that the bandwidth estimate given by (16) is lower than half of the frequency pass-band of the band-pass filter.

The ideal resolution of a conventional force-balancing gyroscope is defined by

$$\sigma = \frac{1}{X_0 \omega_x |T(\omega_x)|} \cdot \left(\int_{\omega_x - BW}^{\omega_x + BW} (|T(j\omega)|^2 S_b + |S(j\omega)|^2 S_p) d\omega \right)^{\frac{1}{2}} \tag{17}$$

where S_p and S_b are, respectively, power spectral density of the position sensing and Brownian noises. In reality, the actual sharpness of the low-pass filter in the demodulation process and aliasing affect resolution performance, and it may be much worse than the estimate given by (17). In the case of the adaptive add-on control, resolution is a function of the adaptation gain γ_Ω and the pass-band of the band-pass filter $F_{\mathrm{BPF}}(s)$. In order to accurately estimate resolution of nominal system, consider the following state-space realization of $T_{\mathrm{BPF}}(s)$ and $S_{\mathrm{BPF}}(s)$:

$$T_{\mathrm{BPF}}(s) : (A_T, B_T, C_T)$$
$$S_{\mathrm{BPF}}(s) : (A_S, B_S, C_S).$$

Then, the (14) and (15) are realized the following state-space form.

$$\begin{bmatrix} \dot{x}_e \\ \dot{\tilde{\theta}} \end{bmatrix} = \begin{bmatrix} A_{11} & A_{12} \\ A_{21} & 0 \end{bmatrix} \begin{bmatrix} x_e \\ \tilde{\theta} \end{bmatrix} + \begin{bmatrix} B_1 \\ 0 \end{bmatrix} \begin{bmatrix} b \\ n \end{bmatrix} \tag{18}$$

TABLE I
KEY PARAMETERS OF THE GYROSCOPE

parameter	value
mass	$5.095 \times 10^{-7} kg$
x-axis frequency	$4.17\ KHz$
Quality factor	40
Brownian noise PSD	$5.53 \times 10^{-24} N^2 sec$
Position noise PSD	$1.49 \times 10^{-27} m^2 sec$

TABLE II
CONTROLLER PARAMETERS FOR THE SIMULATION

$K(s)$	$\frac{100s+70}{s+12}$
$F_{BPF}(s)$	$\frac{7.986s^3}{(s+1.1)^3(s+0.9)^3}$
γ_Ω	0.03
γ_ω	0.05

where

$$A_{11} = diag\{A_T, A_T, A_S\},\ A_{21} = -\gamma v [C_T\ C_T\ C_S]$$
$$A_{12} = \begin{bmatrix} B_T v^T \\ 0 \end{bmatrix},\ B_1 = \begin{bmatrix} 0 & 0 \\ B_T & 0 \\ 0 & B_S \end{bmatrix}$$
$$\gamma = diag\{2\gamma_\Omega, \gamma\omega\},\ v = [\dot{x}\ x]^T.$$

The covariance of $[x_e^T\ \tilde{\theta}^T]^T$ can be computed by solving the following covariance propagation equation:

$$\dot{P} = PA^T + AP + BSB^T \tag{19}$$

where $S = diag\{S_b, S_p\}$. The standard deviation of the angular rate estimate error, or resolution σ_Ω, is obtained from the covariance matrix P, and is computed by

$$\sigma_\Omega = \sqrt{CPC^T} \tag{20}$$

where $C = [0_{1\times m}\ 1]$, and m is a dimension of P. Now, we investigate a relationship of resolution performance between con-

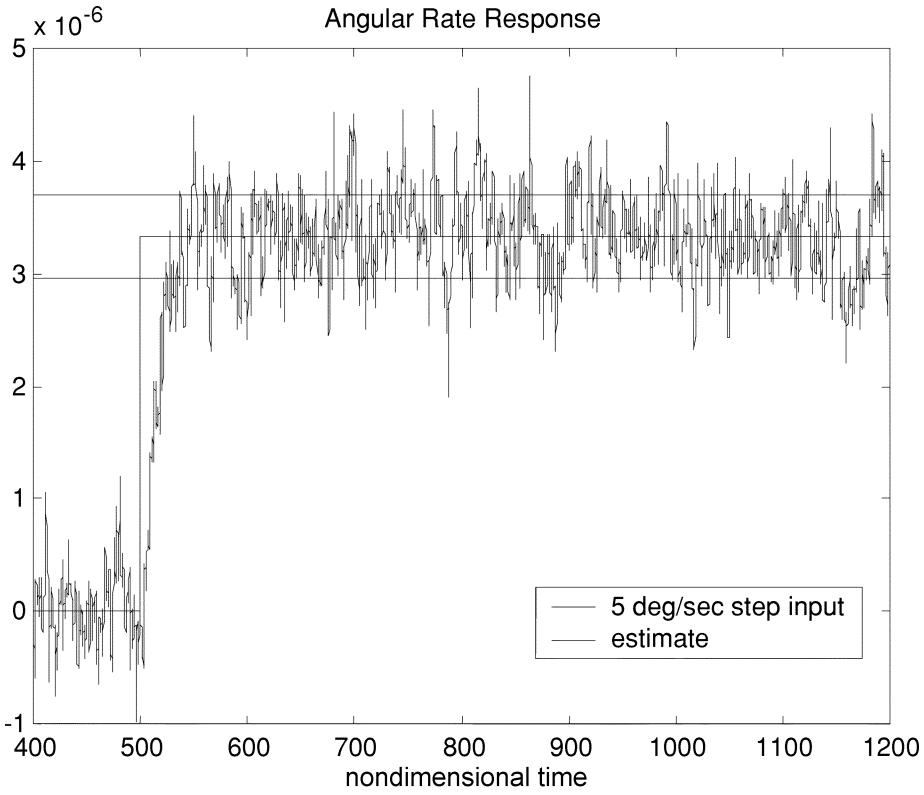

Fig. 5. Time response of angular rate estimate to the 5 deg/s step input.

ventional force-balancing and adaptive add-on force-balancing schemes. If we substitute (11) to (13), then

$$\dot{\tilde{\theta}} = -\gamma v T_{\mathrm{BPF}}(v^T\tilde{\theta}) - \gamma v T_{\mathrm{BPF}}(b) - \gamma v S_{BPF}(n). \quad (21)$$

The stochastic expectation equation of (21) is given by $E[\dot{\tilde{\theta}}] = -\gamma v T_{\mathrm{BPF}}(v^T E[\tilde{\theta}])$, where $E[\cdot]$ denotes stochastic expectation. Define the expectation error as $\check{\theta} = \tilde{\theta} - E[\tilde{\theta}]$, then

$$\begin{aligned}\dot{\check{\theta}} &= -\gamma v T_{\mathrm{BPF}}(v^T\check{\theta}) - \gamma v T_{\mathrm{BPF}}(b) - \gamma v S_{\mathrm{BPF}}(n) \\ &\approx -\gamma v T_{\mathrm{BPF}}(v^T)\check{\theta} - \gamma v T_{\mathrm{BPF}}(b) - \gamma v S_{\mathrm{BPF}}(n) \quad (22)\end{aligned}$$

where we have utilized the assumption that the dynamics of $\check{\theta}$ is slow. Thus, the transfer function from noises to $\check{\theta}$ is given by

$$\begin{aligned}\check{\theta}(s) = &-(sI + \gamma v T_{\mathrm{BPF}}(v^T))^{-1}\gamma v T_{\mathrm{BPF}}(b) \\ &-(sI + \gamma v T_{\mathrm{BPF}}(v^T))^{-1}\gamma v S_{\mathrm{BPF}}(n). \quad (23)\end{aligned}$$

If we assume phase delay $\phi \approx 0$ and consider only the angular rate part, then (23) is simplified as

$$\begin{aligned}\check{\Omega}_z(s) &\approx -\frac{\gamma_\Omega X_0 \omega_x}{s + \gamma_\Omega X_0^2 \omega_x^2 |T_{\mathrm{BPF}}(\omega_x)|} \\ &\quad \times \cos(\omega_x t)(T_{\mathrm{BPF}}(b) + S_{\mathrm{BPF}}(n)) \\ &= -\frac{1}{X_0\omega_x|T_{\mathrm{BPF}}(\omega_x)|}\frac{\mathrm{BW}}{s+\mathrm{BW}} \\ &\quad \times \cos(\omega_x t)(T_{\mathrm{BPF}}(b) + S_{\mathrm{BPF}}(n)). \quad (24)\end{aligned}$$

Equation (24) can be interpreted as follows: The noise that contaminates the angular rate estimate is a low-pass filtered signal of the demodulated noise signals, passed through shaping filters $T_{\mathrm{BPF}}(s)$ and $S_{\mathrm{BPF}}(s)$. These are the same noise properties observed in a conventional force-balancing control using a demodulation process. Therefore, (17) can be also used to calculate the upper estimate of the resolution for the adaptive add-on controlled gyroscope.

Because the shape of the frequency response of $S(s)$ is the inverse of that of $G(s)$, the power of the noise in band-pass filtered control output signal $\tilde{u}_f$ is minimal when $\omega_x = \omega_y$. Thus, the mode tuning problem may be formulated as follows:

$$\omega_y^* = \arg_{\omega_y} \min E[\tilde{u}_f^2] \quad (25)$$

where $E[\cdot]$ stands for the stochastic expectation. Note that the noise properties of the angular rate estimate such as standard deviation can easily be calculated by measuring control output signal $\tilde{u}_f$.

V. Simulations

A simulation study using the preliminary design data of the MIT-SOI MEMS gyroscope was conducted, to test the analytical results and verify the predicted performance of the adaptive add-on controlled gyroscope presented in this paper. We assumed that the drive and sense axis resonant frequencies are matched and the magnitude of quadrature error is 0.1% of nominal resonant frequency. The data of some of the gyroscope parameters in the model is summarized in Table I. The numerical values for the controller used in the simulation is summarized in Table II. Notice that the numerical values in Table II and the simulation results are shown in nondimensional units, which are nondimensionalized based on the proof-mass, length of one micron and the x-axis nominal natural frequency.

The estimate of the angular rate response to the step input angular rate is shown in Fig. 5. In this figure, the upper and lower bounds of the analytically estimated standard deviation are also plotted. The estimated standard deviation with (20) is 0.56 deg/s

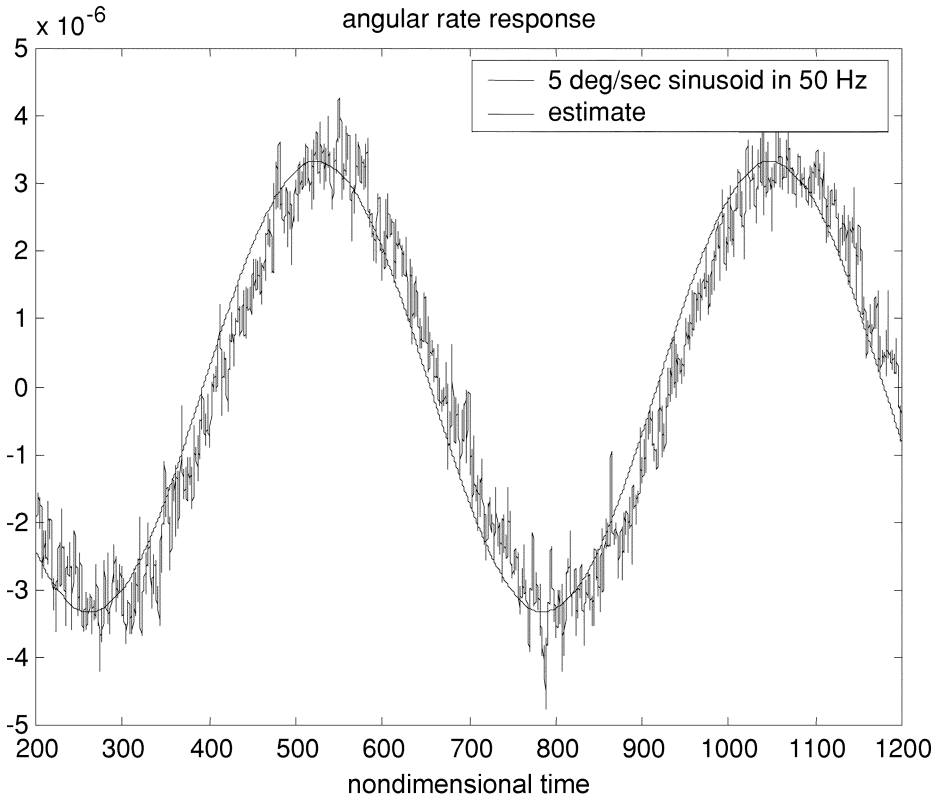

Fig. 6. Time response of angular rate estimate to the 5 deg/s sinusoid input at 50 Hz.

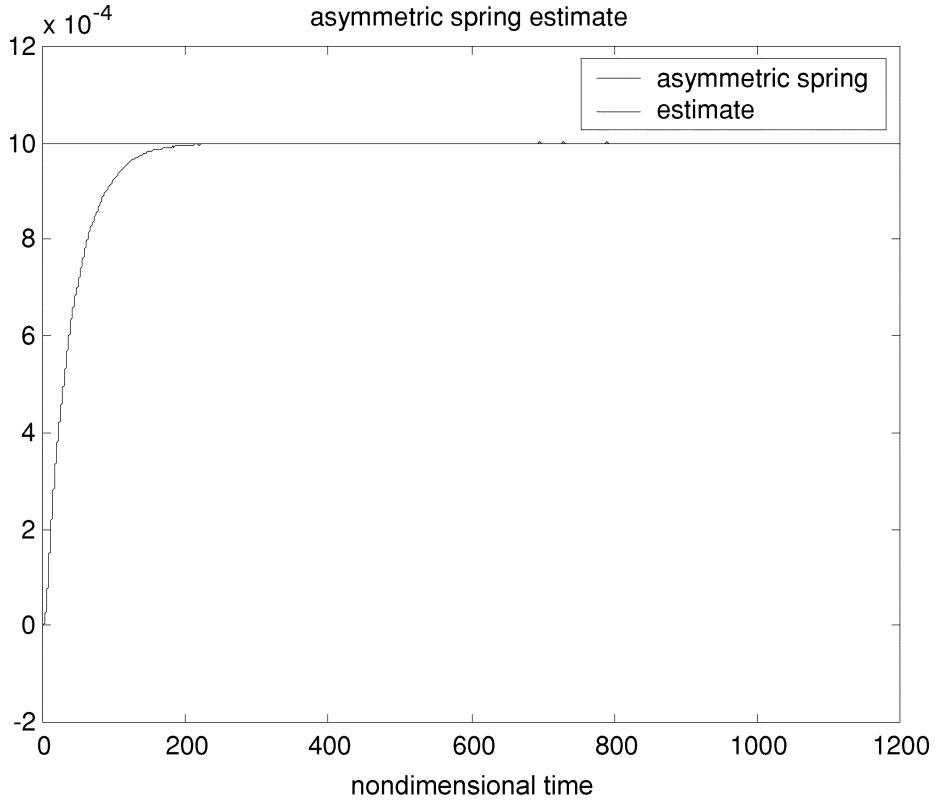

Fig. 7. Time response of quadrature error estimate.

at 50 Hz of bandwidth. Fig. 6 shows the estimate of angular rate response to the sinusoidal input angular rate, and Fig. 7 shows the time response of the quadrature error estimate. These simulation results well match the theoretical results obtained in this paper.

VI. Conclusion

For a closed-loop mode of operation, an adaptive add-on control scheme was proposed. The idea behind this add-on control is to achieve a zero nominal control output in a conventional force-balancing system by adding an additional outer loop. The proposed outer loop is composed of a band-pass filter, a parameter adaptation algorithm, and an algorithm that generates estimates of the gyroscopic inputs and other perturbation inputs due to fabrication defects. This parameter adaptation algorithm estimates the angular rate and, at the same time, identifies and compensates quadrature error, and may permit on-line automatic mode tuning.

The convergence and resolution analysis of the adaptive add-on controlled gyroscope was presented. This analysis shows that the proposed adaptive add-on control scheme prevents the angular rate estimate from being contaminated by the quadrature error, while keeping ideal resolution performance of a conventional force-balancing scheme. Simulation results were presented which corroborate the analytically derived performance. However, both the open-loop and closed-loop modes are inherently sensitive to some types of fabrication imperfections which can be modeled as cross-damping terms, which produce zero-rate output.

References

[1] N. Yazdi, F. Ayazi, and K. Najafi, "Micromachined inertial sensors," *Proc. IEEE*, vol. 86, no. 8, pp. 1640–1659, Aug. 1998.

[2] A. Shkel, R. T. Howe, and R. Horowitz, "Modeling and simulation of micromachined gyroscopes in the presence of imperfection," in *Int. Conf. On Modeling and Simulation of Microsystems*, Puerto Rico, 1999, pp. 605–608.

[3] W. A. Clark, "Micromachined Vibratory Rate Gyroscopes," Doctoral Thesis, U.C. Berkeley, 1997.

[4] T. N. Juneau, "Micromachined Dual Input Axis Rate Gyroscope," Doctoral dissertation, Berkeley, CA, 1997.

[5] P. W. Loveday and C. A. Rogers, "Modification of piezoelectric vibratory gyroscope resonator parameters by feedback control," *IEEE Trans. Ultrason., Ferroelect. Freq. Contr.*, vol. 45, no. 5, pp. 1211–1215, Sept. 1998.

[6] P. Ward, "Electronics for Coriolis Force and Other Sensors," IEEE U.S. Pat. 5 672 949, Sept. 1997.

[7] P. B. Ljung, "Micromachined Gyroscope with Integrated Electronics," Doctoral dissertation, Berkeley, CA, 1997.

[8] S. Chang, M. Chia, P. Castillo-Borelley, W. Higdon, Q. Jiang, J. Johnson, L. Obedier, M. Putty, Q. Shi, D. Sparks, and S. Zarabadi, "An electroformed CMOS integrated angular rate sensor," *Sens. Actuators*, vol. A 66, pp. 138–143, 1998.

[9] X. Jiang, J. Seeger, M. Kraft, and B. E. Boser, "A monolithic surface micromachined Z- axis gyroscope with digital output," in *Proc. IEEE 2000 Symp. VLSI Circuits*, Honolulu, HI, June 2000, pp. 16–19.

[10] A. M. Shkel, R. Horowitz, A. A. Seshia, S. Park, and R. T. Howe, "Dynamics and control of micromachined gyroscopes," in *IEEE Proc. Amer. Control Conf.*, Jun. 1999, pp. 2119–2124.

[11] S. Park, "Adaptive Control Strategies for MEMS Gyroscopes," Doctoral dissertation, Berkeley, CA, 2000.

[12] C. Lu, M. Lamkin, and B. E. Boser, "A monolithic surface micromachined accelerometer with digital output," *IEEE J. Solid-State Circuits*, vol. 30, no. 12, pp. 1367–1373, Dec. 1995.

[13] S. S. Sastry, *Adaptive Control: Stability, Convergence and Robustness.* Englewood Cliffs, NJ: Prentice Hall, 1989.

Sungsu Park (M'02) was born in Taejon, Korea, in 1966. He received the B.S. and M.S. degrees in aerospace engineering from Seoul National University, Seoul, Korea, in 1988 and 1990, respectively, and the Ph.D. degree in mechanical engineering from the University of California at Berkeley in 2000.

He is currently a Postdoctoral Researcher in the PATH program at the University of California at Berkeley. His research interests include estimation theory, fuzzy control, adaptive and robust control with applications to microelectromechanical systems (MEMS), and aerospace systems.

Dr. Park is a member of AIAA.

Roberto Horowitz (M'89) was born in Caracas, Venezuela, in 1955. He received the B.Sc. degree with Highest Honors in Mechanical Engineering from the University of California at Berkeley in 1978 and a Ph.D. degree from the same institution in 1983.

In 1982, he joined the Department of Mechanical Engineering of the University of California at Berkeley, where he is currently a Professor. He teaches and conducts research in the areas of adaptive, learning, nonlinear and optimal control with applications to micro-electro-mechanical systems (MEMS), mechatronics, robotics and intelligent vehicle and highway systems (IVHS).

Dr. Horowitz was a recipient of an 1984 IBM Young Faculty Development Award and a 1987 NSF Presidential Young Investigator Award. He is a Member of the ASME.